

## Testing Natural compounds : *Argania spinosa* Kernels Extract and Cosmetic Oil as Ecofriendly Inhibitors for Steel Corrosion in 1 M HCl

L. Afia<sup>1</sup>, R. Salghi<sup>1,\*</sup>, El. Bazzi<sup>1,2</sup>, L. Bazzi<sup>3</sup>, M. Errami<sup>1</sup>, O. Jbara<sup>4</sup>, S. S. Al-Deyab<sup>5</sup>, B. Hammouti<sup>6</sup>

<sup>1</sup> Ecole Nationale des Sciences Appliquées, Equipe Génie de l'Environnement et de Biotechnologie, B.P 1136, 80000 Agadir, Morocco.

<sup>2</sup> Etablissement Autonome de Contrôle et de Coordination des Exportations, Agadir, Morocco

<sup>3</sup> Faculté des Sciences, Laboratoire Matériaux & Environnement, B.P 8106, 80000 Agadir, Morocco.

<sup>4</sup> GRSPI, Equipe Matériaux Fonctionnels, Université de Reims, B.P 1039, 51687 Reims, France.

<sup>5</sup> Department of Chemistry, College of Science, King Saud University, B.O. 2455, Riyadh 11451, Saudi Arabia

<sup>6</sup> LCAE-URAC18, Faculté des Sciences, Université Mohammed Premier, B.P. 4808, 60046 Oujda, Morocco

\*E-mail: [r\\_salghi@yahoo.fr](mailto:r_salghi@yahoo.fr)

Received: 16 September 2011 / Accepted: 13 October 2011 / Published: 1 November 2011

---

The effect of addition of argan Kernels extract (AKE) and cosmetic argan oil (CAO) on the corrosion of steel in 1M HCl acid has been studied by weight loss measurements, potentiodynamic polarisation and Electrochemical Impedance Spectroscopy (EIS) measurements. The inhibition efficiency was found to increase with inhibitors content to attain 96% and 91% for AKE (at 3g/L) and CAO (at 6g/L) respectively. Data obtained from EIS studies were analyzed to determinate the model inhibition process through appropriate equivalent circuit models. Inhibition efficiency E (%) obtained from the various methods is in good agreement. The temperature effect on the corrosion behaviour of steel in 1M HCl was studied by potentiodynamic technique in the range from 398 to 328 K. The associated activation energy has been determined. The adsorption of natural products on the steel surface was found obey to Langmuir's adsorption isotherm.

---

**Keywords:** Corrosion; Steel; Inhibition; Argan Kernels extract; Unroasted argan oil; Langmuir.

### 1. INTRODUCTION

Corrosion is a fundamental process playing an important role in economics and safety, particularly for metals and alloys. Steel has found wide applications in a broad spectrum of industries

and machinery; despite its tendency to corrosion. Corrosion inhibition of steel therefore is a matter of theoretical as well as practical importance [1–8]. HCl is one of the most important pickling acids, which is widely used in steel and ferrous alloy industry, acid cleaning, acid descaling, oil well acidification and other petrochemical processes [9–11]. Hydrochloric acid is generally used in the pickling processes of metals and alloys [12–14]. To avoid the attack of acid to the bulk metal, inhibitors are generally added. Organic compounds containing heteroatoms are commonly used to reduce the corrosion attack on steel in acidic media. These compounds adsorb on the metal surface, block the active sites on the surface and thereby reduce the corrosion process [15–21]. In recent years, research into the use of low-cost and ecofriendly compounds as corrosion inhibitors for mild steel has intensified [23–45]. Several studies have been carried out on the inhibition of corrosion of metals by plant extract [46, 47], essential oils [48, 49], or purified compounds [50, 51]. We previously reported that Pennyroyal oil [52], Eucalyptus oil [53], Jojoba oil [54], Rosemary oil

[55-57], Artemisia oil [58-60], Lavender oil [61], Menthol derivatives [62], Eugenol and Acetyleneugenol [63], Pulegone [64] and Limonene [65] have been found to be very efficient corrosion inhibitors for steel in acid media. However, the constituents that provide inhibitive action, the mechanisms and the best condition for inhibition are still unclear. The Argan tree, called *Argania spinosa* (L.) Skeels, is a tropical plant, which belongs to the Sapotaceae family. Populations of Morocco traditionally use the fruits of *A. spinosa* to prepare edible oil [66]. It represents the only endemic species of the genus *Argania*. As an important traditional alimentary medicine, *A. spinosa* is a valuable potential for Moroccan. Traditionally, the Argan tree is used for many purposes. In cosmetics, Argan oil is advocated as moisturizing oil, against acne juvenile and flaking of the skin as well as for nourishes the hair [67]. The encouraging results obtained by naturally oils and extracts as corrosion inhibitors of steel in acid solutions permit to test more extracts and oils [68]. The purpose of this paper is to evaluate as corrosion inhibitors cosmetic Argan oil and kernels extract for mild steel in 1M HCl solution by gravimetric method and electrochemical techniques such as potentiodynamic polarisation, linear polarisation and impedance spectroscopy (EIS). The adsorption and inhibition efficiency of these inhibitors were investigated and the thermodynamic parameters in absence and presence of these inhibitors were calculated.

## 2. MATERIALS AND METHODS

### 2.1. Solutions preparation

### 2.2. Argan kernels extract (AKE):

Sample of ground leaves of the kernels of *Argania spinosa* was collected from the area of Biougra located at Chtouka Ait Baha (Morocco) at March month. Stock solution of the plant extract was prepared by grinding the Kernels of *Argania spinosa* to powdery form. A 1 g sample of the powder was refluxed in 100 mL double distilled water for 24 h in 1 M HCl solution (The solution 1M HCl was prepared by dilution of analytical grade 37% HCl with double distilled water).

The refluxed solution was filtered to remove any contamination. This extract was used to study the corrosion inhibition properties and to prepare the required concentrations of as. The solution tests are freshly prepared before each experiment.

### 2.3. *Cosmetic argan oil (CAO):*

The solution tests are freshly prepared before each experiment by adding the oil directly to the corrosive solution.

### 2.4. *Fatty acid methyl esters composition*

The analyses performed for the purpose of this study were carried out in the laboratory of the Autonomous Establishment of Control and Coordination of Export which applies the official methods of analysis for the determination of fatty acid methyl esters (FAME) in oil [69,70]. The fatty acid methyl esters were analyzed with an Agilent Technologies 6890N gas chromatograph equipped with a capillary column (30 m x 0.32 mm; Supelco, Bellefonte, PA, USA) and flame ionization detection. The column was programmed to increase from 135 to 160°C at 2°C/min and from 160 to 205°C at 1.5°C/min; the detection temperature was maintained at 220°C, injector temperature 220 °C. The vector gas was helium at a pressure of 5520 Pa. Peaks were identified by comparing retention times with those of standard fatty acid methyl esters.

### 2.4. *Tocopherols composition*

For the determination of tocopherols compounds a solution of 250 mg oil in 25 mL n-heptane was used for HPLC analysis. The analysis was conducted using a Agilent low pressure gradient system, fitted with a 1100 pump, a Agilent 1100 Fluorescence Spectrophotometer (detector wavelengths for excitation 290 nm, for emission 330 nm). The sample (20 µL) was injected by a Agilent LC -1100 autosampler onto a phase HPLC column 25 cm x 4 mm ID (Merck, Darmstadt, Germany) used with a flow rate of 1 mL/ min and hexane/tetrahydrofuran (98:2, v/v) as mobile phase [71].

### 2.5. *Sterols composition*

Sterol was determined by the method [70]. Sterol composition was evaluated by GLC-FID/capillary column. Briefly, sterols purified from the unsaponifiable matters by HPLC were transformed into their trimethylsilyl ethers counterparts using pyridine, hexamethyldisilazane, and trimethylchlorosilane 9:3:1 (v/v/v). The sterol profile was analysed using a gas-phase chromatograph fitted with a chroma pack CP SIL 8 C B column (30 m x 0.32 mm i.d.) and a flame ionisation detector. The temperature of the injector and detector were both 300 °C. The column temperature was 200 °C and programmed to increase at the rate of 10 °C/min to 270 °C. The carrier gas was dry oxygen-free

nitrogen, and the internal pressure was 8.6 bars. Sterol quantification was achieved by use of an internal 0.2% chloroform solution of  $\alpha$ -cholestanol.

### 2.6. Weight loss measurements

Coupons were cut into  $2 \times 2 \times 0.08 \text{ cm}^3$  dimensions having composition (0.179% C, 0.165% Si, 0.439% Mn, 0.203% Cu, 0.034% S and Fe balance) used for weight loss measurements. Prior to all measurements, the exposed area was mechanically abraded with 180, 320, 800 grades of emery papers. The specimens are washed thoroughly with bidistilled water degreased and dried with ethanol. Gravimetric measurements are carried out in a double walled glass cell equipped with a thermostated cooling condenser. The solution volume is  $80 \text{ cm}^3$ . The immersion time for the weight loss is 8 h at 298 K.

### 2.7. Electrochemical tests

The electrochemical study was carried out using a potentiostat PGZ100 piloted by Voltmaster soft-ware. This potentiostat is connected to a cell with three electrode thermostats with double wall (Tacussel Standard CEC/TH). A saturated calomel electrode (SCE) and platinum electrode were used as reference and auxiliary electrodes, respectively.

Anodic and cathodic potentiodynamic polarization curves were plotted at a polarization scan rate of 0.5mV/s. Before all experiments, the potential was stabilized at free potential during 30 min. The polarisation curves are obtained from  $-800 \text{ mV}$  to  $-400 \text{ mV}$  at 298 K. The solution test is there after de-aerated by bubbling nitrogen. Gas pebbling is maintained prior and through the experiments. In order to investigate the effects of temperature and immersion time on the inhibitor performance, the test were carried out in a temperature range 298–328 K. The electrochemical impedance spectroscopy (EIS) measurements are carried out with the electrochemical system (Tacussel), which included a digital potentiostat model Voltalab PGZ100 computer at  $E_{\text{corr}}$  after immersion in solution without bubbling. After the determination of steady-state current at a corrosion potential, sine wave voltage (10 mV) peak to peak, at frequencies between 100 kHz and 10 mHz are superimposed on the rest potential. Computer programs automatically controlled the measurements performed at rest potentials after 0.5 hour of exposure at 298 K. The impedance diagrams are given in the Nyquist representation.

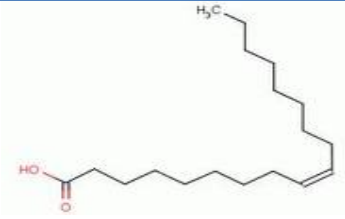
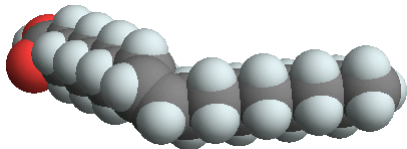
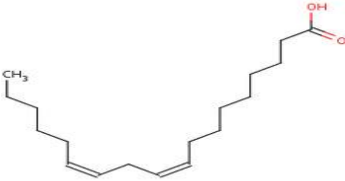
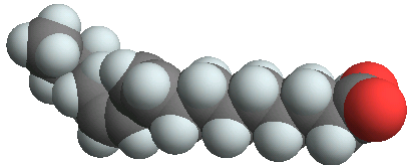
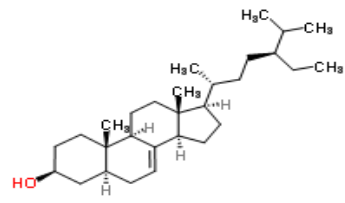
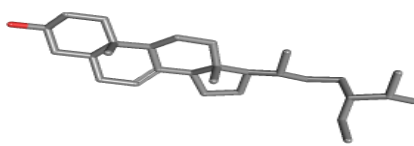
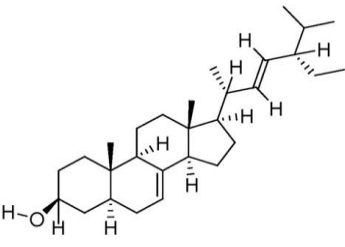
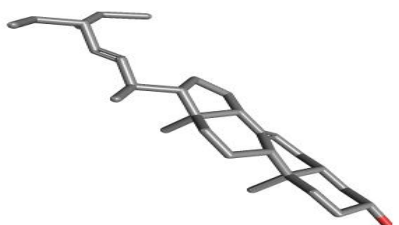
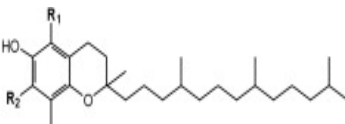

Experiments are repeated three times to ensure the reproducibility.

## 3. RESULTS AND DISCUSSION

### 3.1. Argan oil analysis

The analysis of Argan oil allowed the identification of 24 components which accounted for fatty acid methyl esters (100 %), sterols (93 %) and tocopherols (96.6 %). Their relative percentages are reported in Table 1.

**Table 1.** The systematic (IUPAC) name, 2D and 3D chemical structure of the main constituents of cosmetic argan oil

The constituent	The systematic (IUPAC) name	The 2D chemical structure	The 3D chemical structure
Oleic acid (C18:1)	(Z)-Octadec-9-enoic acid		
Linoleic acid (C18:2)	(9Z, 12Z)-octadeca-9,7-dienoic acid		
Schottenol	(3S,5S,9R,10S,13R,14R,17R)-17-[(2R,5R)-5-ethyl-6-methylheptan-2-yl]-10,13-dimethyl-2,3,4,5,6,9,11,12,14,15,16,17-dodecahydro-1H-cyclopenta[a]phenanthren-3-ol		
Spinasterol	5-alpha-Stigmasta-7,22-dien-3-beta-ol		
$\gamma$ -tocopherol	7,8-trimethyltolcol		

The main constituents were Palmitic acid (13.8 %), Oleic acid (46.3 %), Linoleic acid (32.3 %), Schottenol (48.4 %); Spinasterol (39.1 %) and  $\gamma$ -tocopherol (86.9 %).

3.2. Effect of concentration

3.2.1. Weight loss, corrosion rates and inhibition efficiency

Gravimetric measurements of steel were investigated in 1M HCl in the absence and presence of various concentrations of AKE and CAO at 8 h of immersion and 298 K.

Inhibition efficiency  $E_w$  (%) is calculated as follows:

$$E_w (\%) = \frac{W_{corr} - W'_{corr}}{W_{corr}} \times 100 \tag{1}$$

where  $W_{corr}$  and  $W'_{corr}$  are the corrosion rate of steel in 1M HCl in absence and presence of inhibitor, respectively.

Table 2 summarizes the gravimetric trends of the steel immersed in aerated molar HCl in the absence and the presence of the inhibitors at various concentrations.

**Table. 2.** Effect of AKE & CAO concentration on corrosion data of steel in 1M HCl

Inhibitors	Concentrations (g/l)	$W'_{corr}$ (mg. cm <sup>-2</sup> )	$E_w$ (%)
Blank	0	1.8614	-
kernel Argan extract	0.05	1.1545	38
	0.1	0.6008	68
	0.5	0.5609	70
	1	0.3491	81
	1.5	0.2604	86
	2	0.2115	89
	2.5	0.1110	94
	3	0.0775	96
Cosmetic argan oil	0.1	1.2652	32
	0.5	1.0572	43
	1	0.9008	52
	2	0.5024	73
	3	0.3597	81
	4	0.2801	85
	5	0.2001	89
6	0.1615	91	

It is clear that The corrosion rate decreases with the increase of concentration of the tested inhibitors and in turn the inhibition efficiency ( $E_w$ %) increases to attain 96% and 91% for AKE (at

3g/L) and CAO (at 6g/L) respectively . From weight loss measurements, we can conclude that AKE and CAO are the excellent inhibitors.

3.2.2 Polarization curves

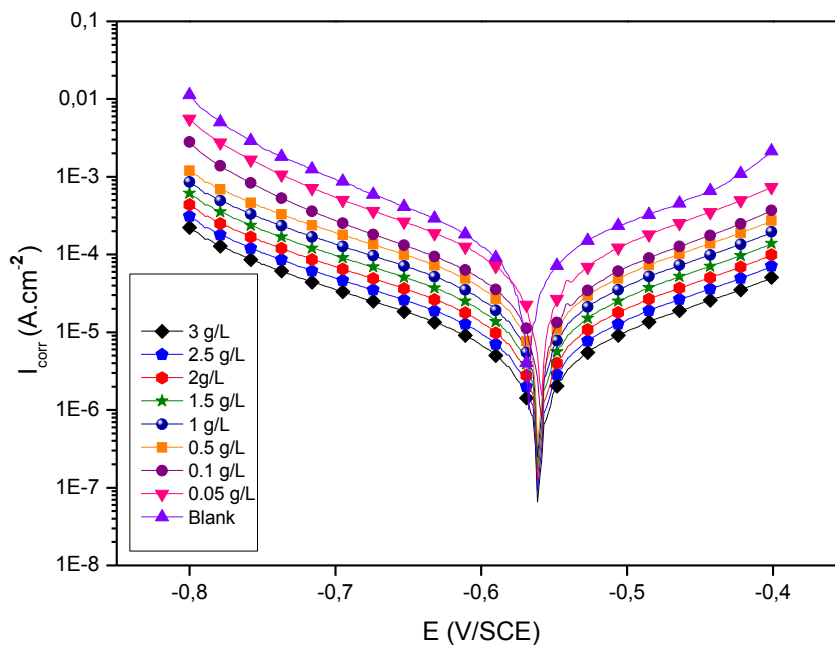


**Figure 1.** Cathodic and Anodic polarisation curves of C38 steel in 1M HCl in the presence of Argan Kernels extract at different concentrations.

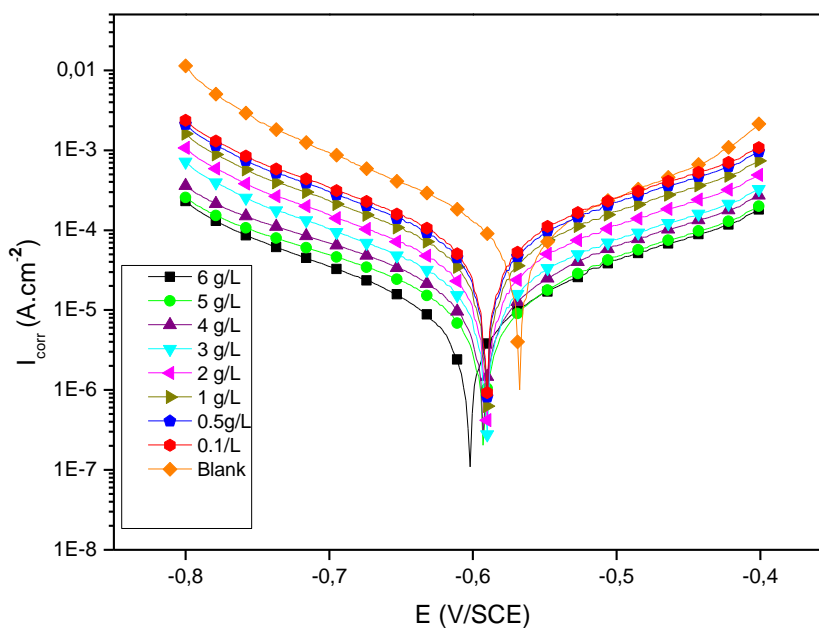


**Figure 2.** Cathodic and Anodic polarisation curves of C38 steel in 1M HCl in the presence of cosmetic argan oil at different concentrations.

Potentiodynamic polarisation curves of steel in 1M HCl in the presence and absence of the tested inhibitors are shown in Figs. 1 and 2. The corrosion parameters including corrosion current densities ( $I_{\text{corr}}$ ), corrosion potential ( $E_{\text{corr}}$ ), cathodic Tafel slope ( $\beta_c$ ), anodic Tafel slope ( $\beta_a$ ) and inhibition efficiency ( $E_I$  %) are listed in Table 3.

**Table 3.** Electrochemical parameters of steel at various concentrations of AKE and CAO respectively in 1M HCl and the corresponding inhibition efficiency.

Inhibitors	Concentrations (g/l)	$E_{\text{corr}}$ (mV/SCE)	$I_{\text{corr}}$ ( $\mu\text{A}/\text{cm}^2$ )	$-\beta_c$ (mV/dec)	$\beta_a$ (mV/dec)	E (%)
Blank	0	-616	94	99	108	-
Kernel argan extract	0.05	-559	59	126	123	37
	0.1	-560	30	103	107	68
	0.5	-562	27	122	118	71
	1	-560	18	137	128	81
	1.5	-558	13	122	119	86
	2	-561	10	138	128	89
	2.5	-561	7	119	117	93
	3	-559	3	134	128	97
Cosmetic argan oil	0.1	-591	64	137	148	32
	0.5	-590	54	133	140	43
	1	-593	45	135	145	52
	2	-591	28	107	118	70
	3	-591	17	130	138	82
	4	-593	14	146	143	85
	5	-593	11	149	126	88
6	-603	8	131	140	91	

In this case, the inhibition efficiency is defined as follows:

$$E\% = \left(1 - \frac{I'_{\text{corr}}}{I_{\text{corr}}}\right) \times 100 \quad (2)$$

Where  $I_{\text{corr}}$  and  $I'_{\text{corr}}$  are, respectively, the uninhibited and inhibited current density respectively.

The corrosion current density was calculated from the intersection of cathodic and anodic Tafel line.

The examination of Fig. 1 and 2 shows that the addition of AKE and CAO affects both anodic dissolution of steel and cathodic reduction reactions indicating that the two compounds could be classified as mixed-type inhibitors. The values of corrosion potential ( $E_{\text{corr}}$ ) remain almost constant upon the addition of inhibitor concentration [72]. We also remark that the cathodic current–potential curves give rise to parallel Tafel lines, which indicate that hydrogen evolution reaction is activation



controlled and that the addition of the APE does not affected the mechanism of this process (Fig.1 & 2) [73].

Inspections of the electrochemical parameter values given in Table. 1, reveal that, inhibition efficiency increases with an increase of the concentration of inhibitors. The maximum inhibition efficiency observed at higher inhibitor concentration indicates that more inhibitor molecules are adsorbed on the metal surface. These compounds are then acting as adsorption inhibitors. We note that the corrosion current densitie were more significantly reduced in the presence of AKE than CAO. The best efficiencies obtained in the presence of AKE and CAO respectively are 97% at 3g/L and 91g/L at 6g/L.

### 3.3. Electrochemical impedance spectroscopy measurements

The corrosion behaviour of steel, in acidic solution in the presence and absence of inhibitors, is investigated by the electrochemical impedance spectroscopy (EIS) at 298 K after 30 min of immersion. Fig. 3 and 4 show the EIS diagrams carried out at 298 K in acid solution with and without AKE and CAO respectively. The impedance parameters derived from these investigations are mentioned in Table 4.

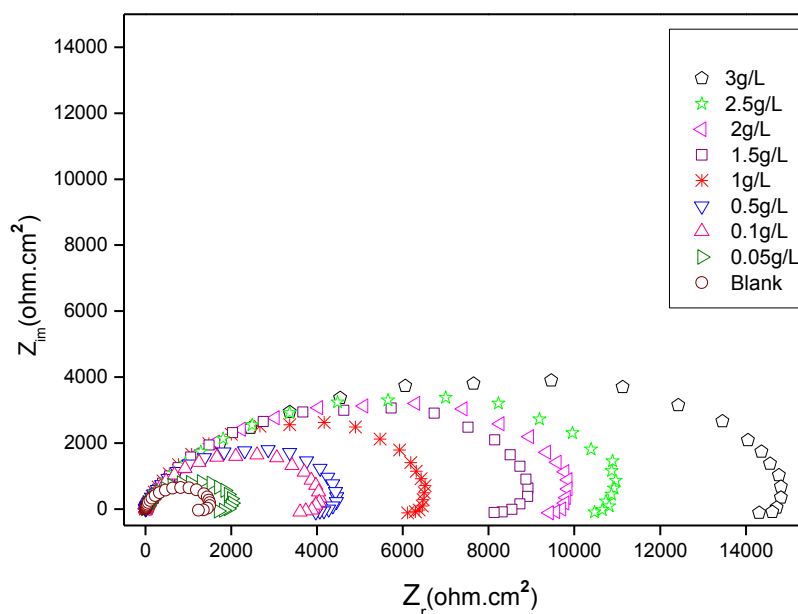


**Figure 3.** Nyquist diagrams for steel electrode with and without kernel Argan extract after 30min of immersion.

The values of inhibition efficiency were calculated using the relation:

$$E_{Rt} \% = \frac{(R_t - R_t^{\circ})}{R_t} \times 100 \tag{3}$$

Here  $R_t$  and  $R_t^0$  are the charge transfer resistances in inhibited and uninhibited solutions respectively.

The charge transfer resistance ( $R_t$ ) values are calculated from the difference in impedance at lower and higher frequencies, as suggested by Tsuru et al [74]. The double layer capacitance ( $C_{dl}$ ) and the frequency ( $f_{max}$ ) at which the imaginary component of the impedance is maximal ( $-Z_{max}$ ) are found as represented in equation:

$$C_{dl} = \left( \frac{1}{\omega R_t} \right) \quad \text{with} \quad \omega = 2\pi f_{max} \quad (4)$$

where  $C_{dl}$ : Double layer capacitance ( $\mu\text{F} \cdot \text{cm}^{-2}$ );  $f_{max}$ : maximum frequency (Hz) and  $R_t$ : Charge transfer resistance ( $\Omega \cdot \text{cm}^2$ )

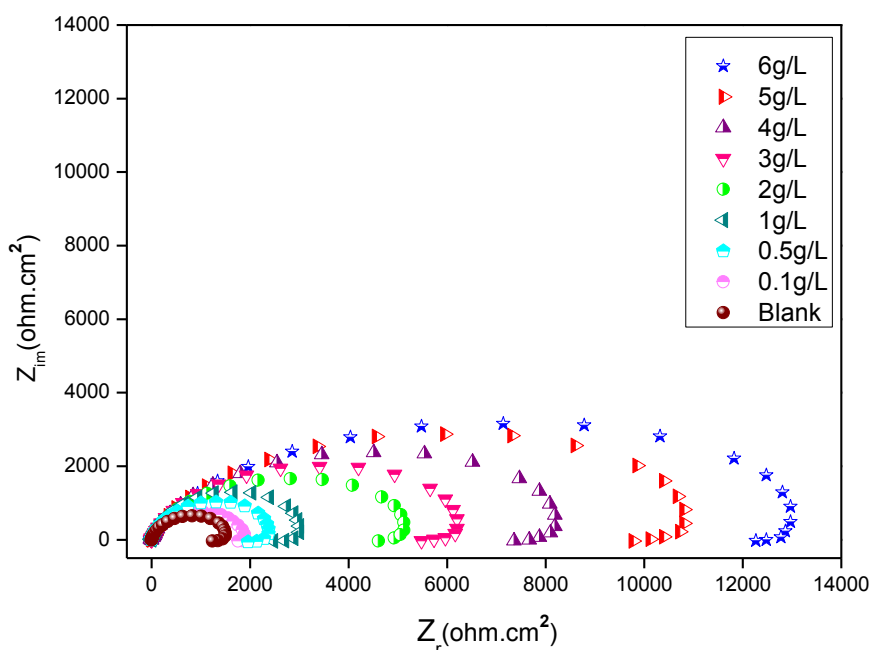


**Figure 4.** Nyquist diagrams for steel electrode with and without cosmetic Argan oil after 30min of immersion.

It is worthy noting that, the presence of inhibitors does not alter the profile of impedance diagrams which are almost semi-circular (Fig. 5 & 6), indicating a charge transfer process mainly controls the corrosion of steel. Deviations of perfect circular shape are often referred to the frequency dispersion of interfacial impedance. This anomalous phenomenon may be attributed to the inhomogeneity of the electrode surface arising from surface roughness or interfacial phenomena [75, 76]. When there is non-ideal frequency response, it is common practice to use distributed circuit elements in an equivalent circuit. The most widely employed is the constant phase element (CPE). In general, a CPE is used in a model in place of a capacitor to compensate for inhomogeneity in the system [77].

In order to fit and analyze the EIS data, an equivalent circuit was selected and is shown in Fig. 5. This circuit is generally used to describe the iron/acid interface model [78]. Excellent fit with this model was obtained with our experimental data. As an example, the Nyquist and Bode plot for AKE at 0.1g/L in 1M HCl are presented in fig. 6a and 6b, respectively.

**Table 4.** Impedance parameters for corrosion of steel in acid at various contents of AKE and CAO respectively

Inhibitors	Concentrations (g/L)	$R_t(k\Omega.cm^2)$	$f_{max}(Hz)$	$C_{dl}(\eta F/cm^2)$	$E_{RT}(\%)$
Blank	0	2.43	50	148.62	-
Kernel Argan extract	0.05	34.82	49	93.32	38
	0.1	71.43	47.5	46.93	70
	0.5	77.68	45.1	45.45	72
	1	115.18	42	32.92	81
	1.5	157.14	33.4	30.34	86
	2	175.00	31	29.35	88
	2.5	223.21	29	24.60	90
	3	285.71	28	19.90	9
Cosmetic argan oil	0.1	33.04	46.4	103.88	35
	0.5	39.29	46	88.11	45
	1	46.43	44.5	77.07	54
	2	83.93	42.3	44.85	74
	3	115.18	40	34.56	81
	4	150.00	36	29.49	86
	5	198.21	30.1	26.69	89
	6	235.71	29	23.29	91

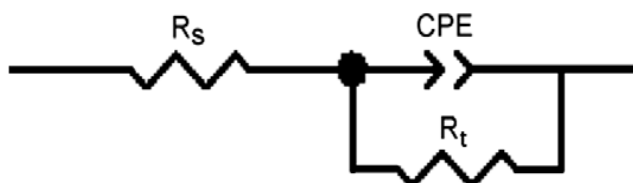


**Figure 5.** Electrochemical equivalent circuit used for impedance spectra of AKE and CAO.

In this equivalent circuit,  $R_s$  is the solution resistance,  $R_t$  is the charge transfer resistance and CPE is a constant phase element. The impedance function of the CPE is as follows:

$$Z_{CPE} = Y^{-1} (j\omega)^{-n} \tag{5}$$

Where  $Y$  is the magnitude of CPE,  $x$  is the angular frequency ( $2\pi f_{max}$ ), and the deviation parameter  $n$  is a valuable criterion of the nature of the metal surface and reflects microscopic fluctuations of the surface. For  $n = 0$ ,  $Z_{CPE}$  represents a resistance with  $R = Y^{-1}$ ;  $n = -1$  an inductance with  $L = Y^{-1}$ ,  $n = 1$  an ideal capacitor with  $C = Y$  [79].

The idealized capacitance ( $C_{id}$ ) values can be described by CPE parameter values  $Y$  and  $n$  using the following expression [80]:

$$C_{id} = Y\omega^{n-1} / \sin(n\pi/2) \tag{6}$$

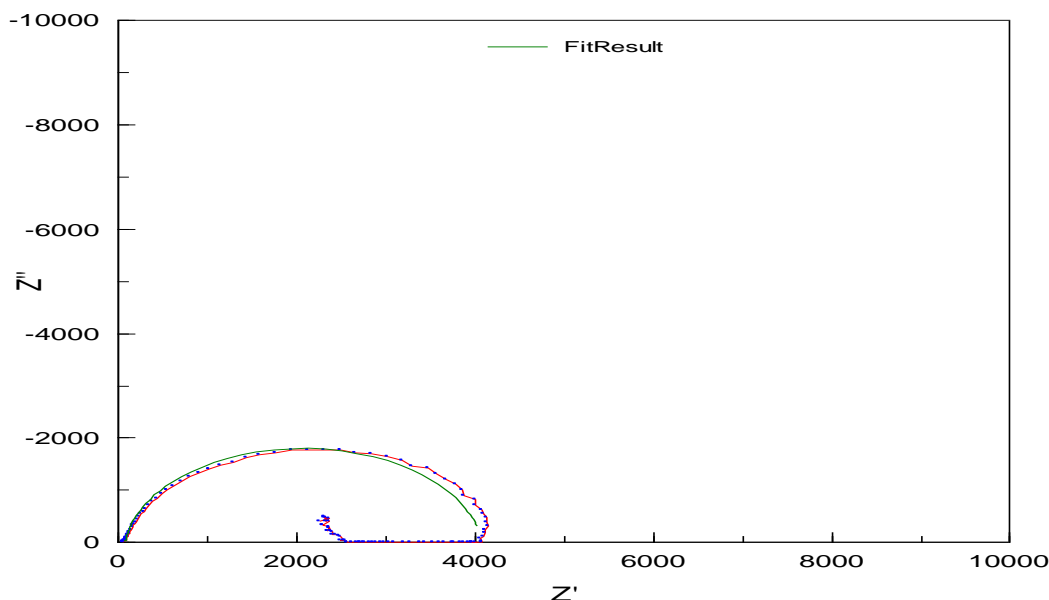


**Figure 6a:** EIS Nyquist plot for mild steel /1M HCl+0.1g/L AKE interface: — experimental data  
— calculated

The measured and simulated data fit very well. It is observed that the fitted data follow almost the same pattern as the original results along the whole diagrams, with an average error about 1% in all cases.  $R_t$  values were simultaneously determined by analysis of the complex-plane impedance plots and the equivalent circuit model. Also, It was found that  $R_t$  values increased with increasing inhibitors concentration (AKE & CAO).

The general shape of the curves is very similar for all samples; the shape is maintained throughout the whole concentrations, indicating that almost no change in the corrosion mechanism occurred due to the inhibitors addition [81].

The examination of the EIS parameters shows that the value of  $R_t$  increases with increase in the concentration of the inhibitors (AKE & CAO), Values of double layer capacitance are also brought down to the maximum extent in the presence of inhibitor and the decrease in the values of  $C_{dl}$  follows the order similar to that obtained for  $I_{corr}$  in this study. It

has been reported that the adsorption process on the metal surface is characterized by a decrease in  $C_{dl}$  [74]. The best efficiencies obtained in the presence of AKE and CAO respectively are 93% at 3g/L and 91g/L at 6g/L.

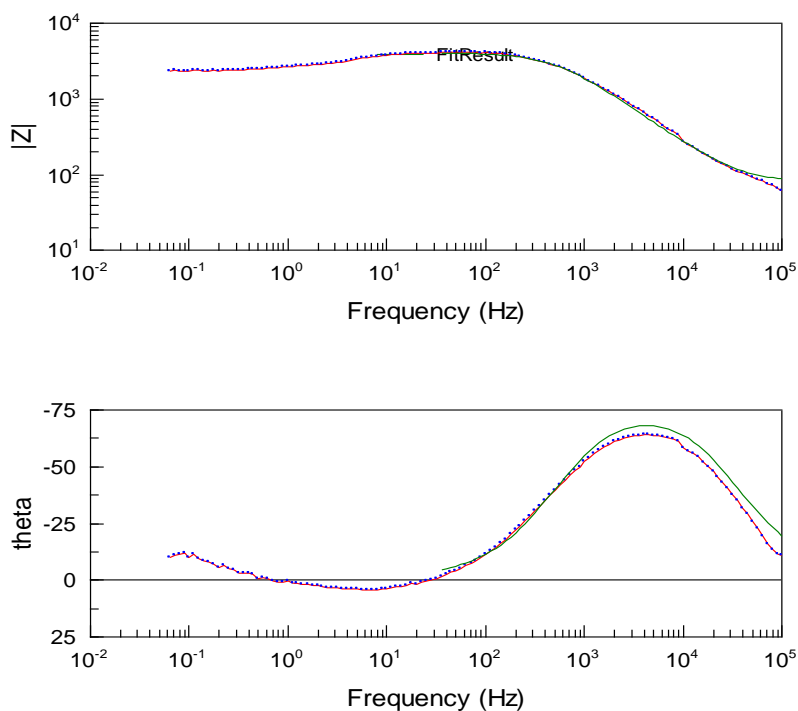


**Figure 6b:** EIS Bode plot for mild steel /1M HCl+0.1g/L AKE interface: — experimental data  
— calculated

The results obtained from the polarization technique were in good agreement with those obtained from the electrochemical impedance spectroscopy (EIS) and gravimetric method with a small variation.

### 3.3. Effect of temperature

#### 3.3.1. Polarization curves

Temperature has a great effect on the corrosion phenomenon. Generally the corrosion rate increases with the rise of the temperature. For this purpose, we made potentiodynamic polarization in the range of temperature 298 to 328 K, in the absence and presence of AKE and CAO at 1g/L and 3g/L respectively. The corresponding data are shown in fig 7, 8, 9 and Table 5.

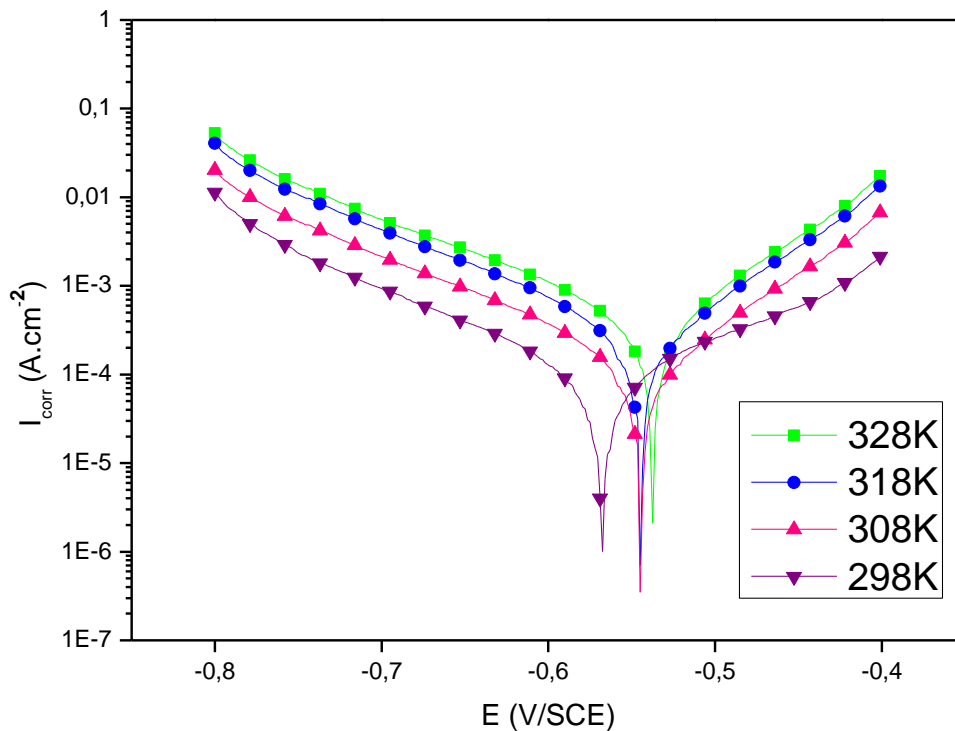


Figure 7. Potentiodynamic polarisation curves of C38 steel in 1M HCl at different temperatures

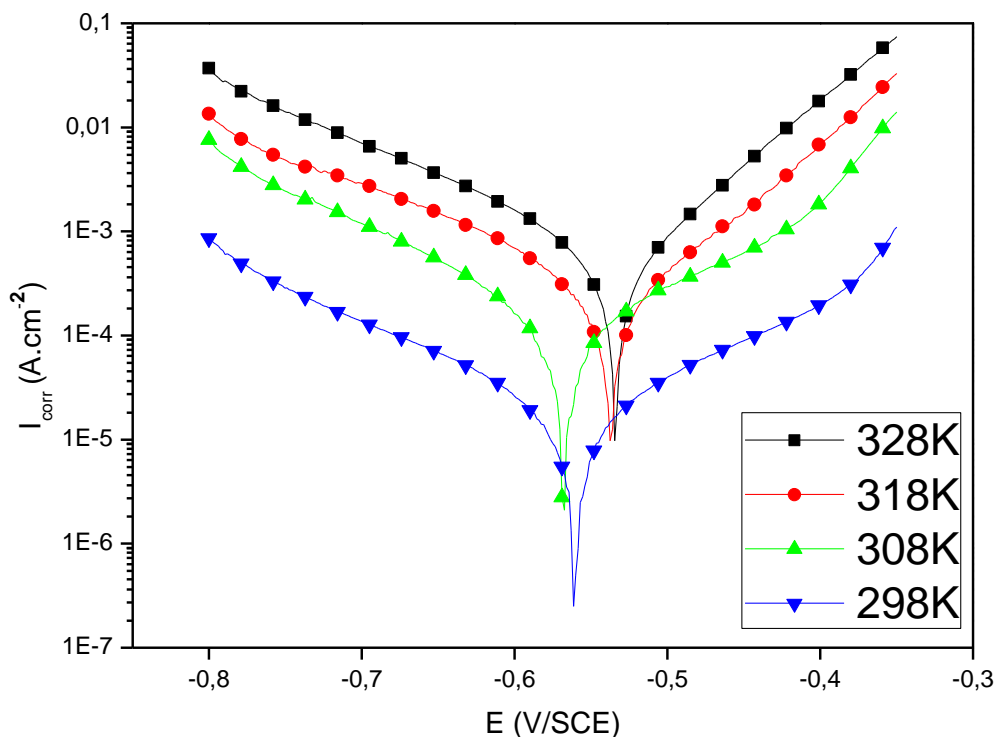
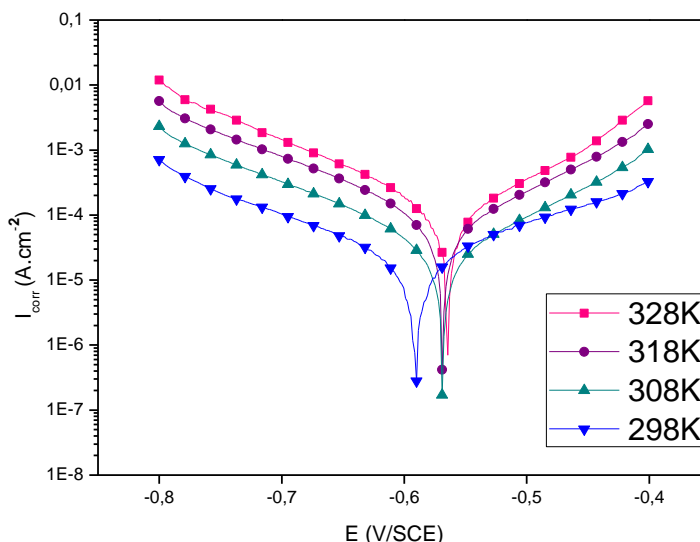


Figure 8. Potentiodynamic polarisation curves of C38 steel in 1M HCl in the presence of 1g/L of AKE at different temperatures.



**Figure 9.** Potentiodynamic polarisation curves of C38 steel in 1M HCl in the presence of 3g/L of CAO at different temperatures.

It is clear from fig. 7 and table 6 that the increase of corrosion rate is more pronounced with the rise of temperature for blank solution.

In the presence of AKE (fig. 8 and table 5), corrosion rate increases strongly at high temperatures. It can be deduced that AKE becomes a catalyst compound from 308 K. This result was confirmed by weight loss measurement and EIS method.

As seen from fig. 9 and table 5 in the presence of CAO,  $I_{corr}$  is highly reduced. Also, the inhibition efficiency decreases slightly with increasing temperature. This can be explained by the decrease of the strength of adsorption processes at elevated temperature and suggested a physical adsorption mode [82]. From this result, we can conclude that CAO is a good inhibitor.

**Table 5.** Effect of temperature on the steel in free acid and at 1g/L and 3g/ L of AKE and CAO respectively

Inhibitors	Temperature (K)	$E_{corr}$ (mV/SCE)	$I_{corr}$ ( $\mu A/cm^2$ )	$-b_c$ (mV/dec)	$b_a$ (mV/dec)	E (%)
Blank	298	-616	94	99	108	-
	308	-544	157	126	68	-
	318	-545	305	129	75	-
	328	-537	399	136	78	-
Kernel Argan extract	298	-560	18	137	128	81
	308	-568	166	125	93	- 6
	318	-536	338	173	81	- 11
	328	-534	756	140	74	- 89
Cosmetic argan oil	298	-591	18	130	138	81
	308	-568	37	136	96	76
	318	-570	93	116	101	70
	328	-565	128	117	93	68

3.3.2. Kinetic parameters

The activation energies of corrosion process in free and inhibited acid were calculated using Arrhenius equation (7):

$$I_{corr} = A \exp\left(-\frac{E_a}{RT}\right) \tag{7}$$

Where A is Arrhenius factor,  $E_a$  is the apparent activation corrosion energy, R is the perfect gas constant and T the absolute temperature.

Plotting ( $\log I_{corr}$ ) versus  $1/T$  gives straight lines as revealed from Fig. 10.

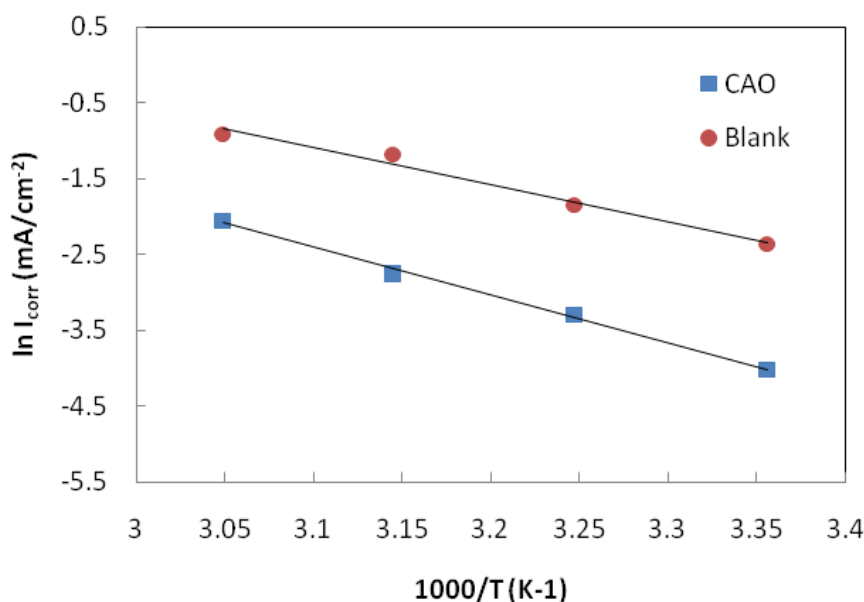


**Figure 10.** Arrhenius plots of steel in 1 M HCl with and without 3 g/L of CAO

The activation energy values obtained are 52 and 41 kJ/mol for 3g/L of CAO and free acid, respectively.

It's observed that  $E_a$  increases slightly in the presence of CAO that indicates the good performance of this inhibitor at higher temperatures. Generally, the inhibitive additives cause a rise in activation energy value when compared to the blank and this could be often interpreted as an indication for the formation of an adsorptive film by a physical (electrostatic) mechanism [83,84].

Kinetic parameters, such as enthalpy and entropy of corrosion process, may be evaluated from the effect of temperature. An alternative formulation of Arrhenius equation is (8) [85]:

$$I_{corr} = \frac{RT}{Nh} \cdot \exp\left(\frac{\Delta S^*}{R}\right) \cdot \exp\left(-\frac{\Delta H^*}{RT}\right) \tag{8}$$



Where N is the Avogadro’s number, h the Plank’s constant, R is the perfect gas constant,  $\Delta S^*$  and  $\Delta H^*$  the entropy and enthalpy of activation, respectively.

Fig. 11 shows a plot of  $\ln(W/T)$  against  $1/T$  for CAO. Straight lines are obtained with a slope of  $(-\Delta H^*/R)$  and an intercept of  $(\ln R/Nh + \Delta S^*/R)$  from which the values of  $\Delta H^*$  and  $\Delta S^*$  are calculated respectively (Table 6).

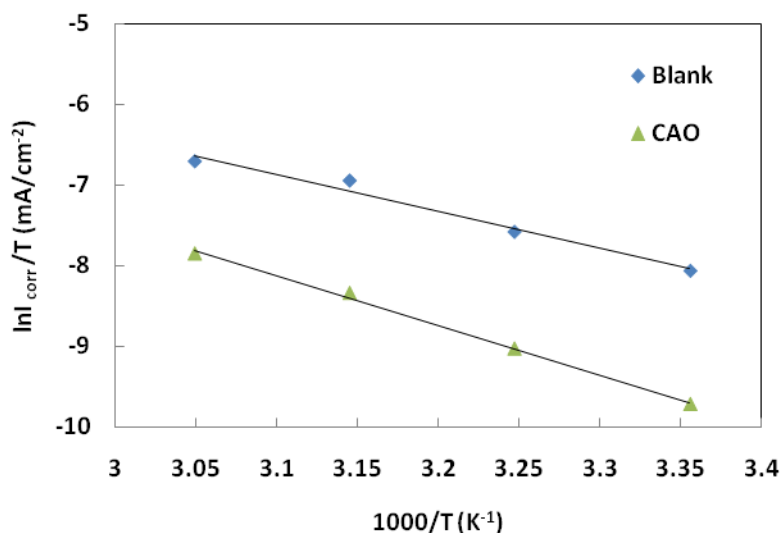


**Figure 11.** Relation between  $\ln(W_{corr}/T)$  and  $1000/T$  in acid at different temperatures .

The value of free energy  $\Delta G^*$  is deduced from the formula (9):

$$\Delta G^* = \Delta H^* - T\Delta S^* \tag{9}$$

**Table 6.** The values of activation parameters  $\Delta H^*$ ,  $\Delta S^*$  and  $\Delta G^*$  for mild steel in 1M HCl in the absence and the presence of 3 g/L of CAO respectively.

Inhibitors	$\Delta H^*$ (kJ/mole)	$\Delta S^*$ (J/mole <sup>-1</sup> .k <sup>-1</sup> )	$\Delta G^*$ (kJ/mole à T=298K)
<b>Blank</b>	38	-136	78
<b>Untroasted argan oil ( 3g/L )</b>	51	-106	83

From the data obtained in Table 6, it can be concluded that:

\* The signs of the enthalpies  $\Delta H^*$  reflect the endothermic nature of the steel dissolution process.

\* The Large and negative value of entropy in the presence of CAO imply that the activated complex in the rate determining step represents an association rather than a dissociation step, meaning that a decrease in disordering takes place on going from reactants to the activated complex [86, 87] .

\* The  $\Delta G^*$  values for inhibited systems were more positive than that for the uninhibited systems revealing that in presence of inhibitor addition the activated corrosion complex becomes less stable as compared to its absence.

### 3.3.3. Adsorption isotherm

Additional information about the properties of the tested compounds may be provided from the kind of adsorption isotherm. Several adsorption isotherms were tested and the Langmuir adsorption isotherm was found to provide best description of the adsorption behaviour of the investigated inhibitor. The Langmuir isotherm is given by the equation (10) [88]:

$$\frac{C}{\theta} = \frac{1}{K} + C \quad \text{with } K = \frac{1}{55.5} \exp\left(-\frac{\Delta G_{\text{ads}}}{RT}\right) \quad (10)$$

Where C is the inhibitor concentration,  $\theta$  the fraction of the surface covered determined by  $E/100$ , k the equilibrium constant,  $\Delta G_{\text{ads}}$  is the standard free energy of adsorption reaction, R is the universal gas constant, T is the thermodynamic temperature and the value of 55.5 is the concentration of water in the solution in mol/L. Figs. 12 and 13 show the dependence of the ratio  $C/\theta$  as function of C for AKE and CAO respectively.

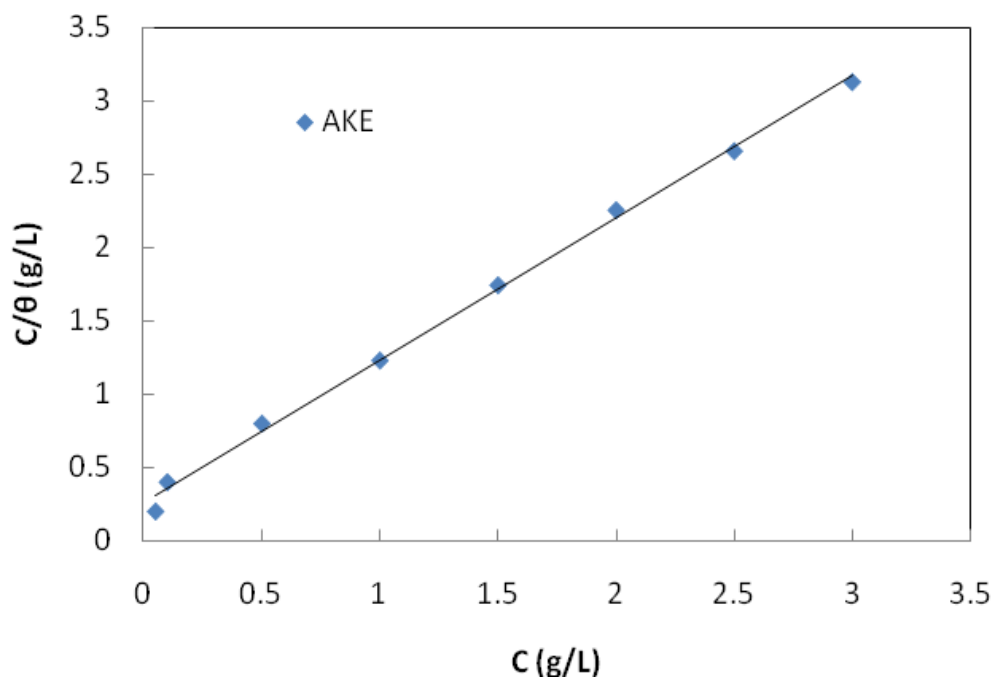


**Figure 12.** Plots of Langmuir adsorption isotherm of AKE on the steel surface at 298K.

If we assume that the major component plays the principal role in inhibition, then adsorption obeys to Langmuir isotherm. But, generally in this kind of green inhibitors (natural plants: oil or

extract), inhibitory action is related to the intermolecular synergistic effect if the various components of natural oil or extract [89]. It is safely recommended to not determine  $\Delta G_{\text{ads}}$  values since the mechanism of adsorption remains unknown.

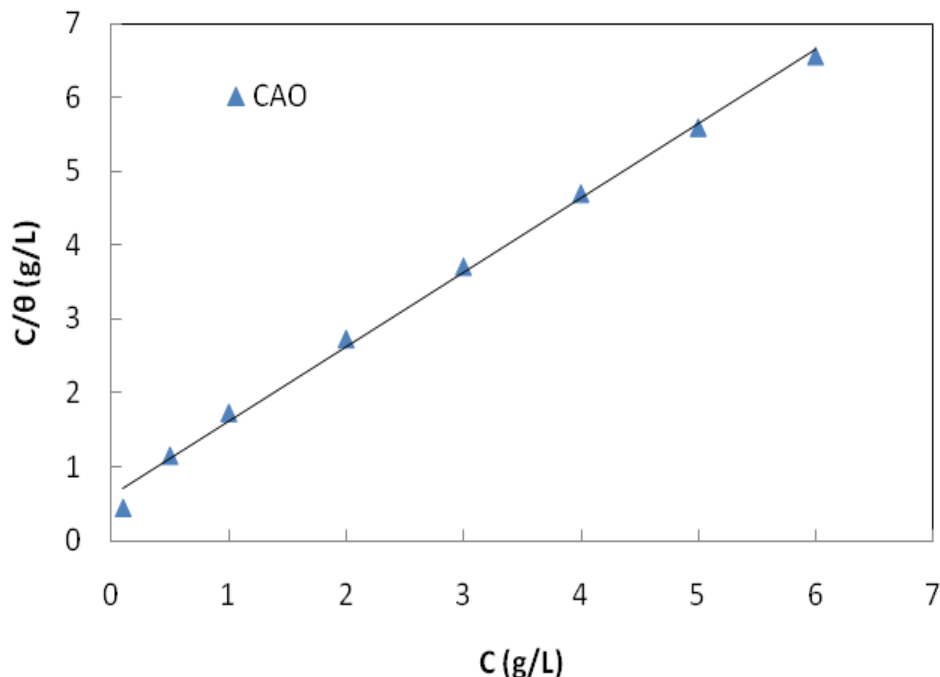


**Figure 13.** Plots of Langmuir adsorption isotherm of CAO on the steel surface at 298K.

#### 4. CONCLUSION

In this work we have studied the corrosion inhibition of cosmetic argan oil and kernels extract for mild steel in 1M HCl solution by gravimetric method and electrochemical techniques such as potentiodynamic polarization. The results obtained are in good agreement and are given as follows.

\* AKE and CAO act as mixed type inhibitors without modifying the mechanism of hydrogen evolution.

\* The inhibition efficiency of AKE and CAO increases with the increase of inhibition concentration to reach 97% at 1g/L of AKE and 91% at 6g/L of CAO.

\* The data obtained from the three different methods: potentiodynamic polarisation, EIS and weight loss, are in good agreements.

\*Data obtained from EIS studies were analyzed to determinate the model inhibition process through appropriate equivalent circuit models.

\* The inhibition efficiency of AKE and CAO decreases with the rise of temperature.

\* AKE and CAO are adsorbed on the steel surface according to the Langmuir adsorption isotherm. Thermodynamic parameters are determined.

\* AKE and CAO being natural and environmentally benign products, they can be used as an alternative for toxic chemical inhibitors in acidization and acid pickling of mild steel.

#### ACKNOWLEDGEMENTS

The authors wish to thank the North Atlantic Treaty Organization (NATO) program (CBP.MD.CLG 983108) and Volubilis MA/10/226 for supporting this work. Prof S. S. Deyab and Prof B. Hammouti extend their appreciation to the Deanship of Scientific Research at King Saud University for funding the work through the research group project.

#### References

1. Z. Wahbi, A. Guenbour, H. Abou El Makarim, A. Ben Bachir, S. El Hajjaji, *Prog. Org. Coat.* 60 (2007) 224.
2. K.F. Khaled, *Electrochim. Acta*, 53 (2008) 3484.
3. K.F. Khaled, *Appl. Surf. Sci.* 252 (2006) 4120.
4. M.A. Amin, S.S. Abd El Rehim, H.T.M. Abdel-Fatah, *Corros. Sci.* 51 (2009) 882.
5. S.S. Abdel Rehim, O.A. Hazzazi, M.A. Amin, K.F. Khaled, *Corros. Sci.* 50 (2008) 2258.
6. H.H. Hassan, E. Abdelghani, M.A. Amin, *Electrochim. Acta* 52 (2007) 6359.
7. M.A. Amin, S.S. Abd El Rehim, E.E.F. El-Sherbini, R.S. Bayoumi, *Electrochim. Acta* 52 (2007) 3588.
8. K.F. Khaled, M.A. Amin, *Corros. Sci.* 51 (2009) 1964.
9. A.O. James, N.C. Oforika, K. Abiola, *Int. J. Electrochem. Sci.* 2 (2007) 284.
10. E.E. Ebenso, *Niger. J. Chem. Res.* 6 (2001) 12.
11. U.J. Ekpe, P.C. Okafor, E.E. Ebenso, O.E. Offiong, B.I. Ita, *Bull. Electrochem.* 17 (2001) 135.
12. S.A. Abd El-Maksoud, A.S. Fouda, *Materials Chemistry and Physics* 93 (2005) 84–90.
13. M.A. Migahed, I.F. Nassar, *Electrochimica Acta* 53 (2008) 2877–2882.
14. M.A. Migahed, M. Abd-El-Raouf, A.M. Al-Sabagh, H.M. Abd-El-Bary, *Electrochim. Acta* 50 (2005) 4683.
15. M. Scendo, *Corros. Sci.* 49 (2007) 3953.
16. M. Benabdellah, A. Aouniti, A. Dafali, B. Hammouti, M. Benkaddour, A. Yahyi, A. Et-Touhami, *Appl. Surf. Sci.* 252 (2006) 8341.
17. K.C. Pillai, R. Narayan, *Corros. Sci.* 23 (1983) 151.
18. K. Laarej, H., Abou El Makarim, L. Bazzi, R. Salghi, B. Hammouti, *Arab. J. Chem.* 3 (2010) 55.
19. M. Bouklah, N. Benchat, A. Aouniti, B. Hammouti, M. Benkaddour, M. Lagrenee, H. Vezine, F. Bentiss, *Prog. Org. Coat.* 51 (2004) 118.
20. A. Chetouani, B. Hammouti, A. Aouniti, N. Benchat, T. Benhadda, *Prog. Org. Coat.* 45 (2002) 373.
21. F. Touhami, A. Aouniti, Y. Abed, B. Hammouti, S. Kertit, A. Ramdani, K. Elkacemi, *Corros. Sci.* 42 (2000) 929.
23. I.H. Farooqi, A. Hussain, M.A. Quraishi, P.A. Saini, *Anti-Corros. Meth. Mater.* 46 (1999) 328.
24. A.Y. El-Etre, *Corros. Sci.* 40 (1998) 1845.
25. A.Y. El-Etre, M. Abdallah, *Corros. Sci.* 42 (2000) 731.
26. A.Y. El-Etre, *Corros. Sci.* 43 (2001) 1031.
27. A.Y. El-Etre, M. Abdallah, Z.E. El-Tantawy, *Corros. Sci.* 47 (2004) 385.
28. A.Y. El-Etre, *Appl. Surf. Sci.* 252 (2006) 8521.
29. Y. Li, P. Zhao, Q. Liang, B. Hou, *Appl. Surf. Sci.* 252 (2005) 1245.
30. A.Y. El-Etre, *Corros. Sci.* 45 (2003) 2485.

31. A.J. Altwaiq, S. Khouri, S. Al-luaibi, R. Lehmann, H. Drücker, C. Vogt, *J. Mater. Environ. Sci.* 2 (2011) 259.
32. P.B. Raja, M.G. Sethuraman, *Pigment Resin Technol.* 38 (2009) 33.
33. P.B. Raja, M.G. Sethuraman, M. Gopalakrishnan, *Mater. Lett.* 62 (2008) 113.
34. K.S. Parikh, K.J. Joshi, *Trans. SAEST* 39 (2004) 29.
35. A.Y. El-Etre, *Bull. Electrochem.* 22 (2006) 75.
36. M. Lebrini, F. Robert, C. Roos, *Int. J. Electrochem. Sci.*, 6(2011)847
37. J.C. da Rocha, J.A.C.P. Gomes, E. D'Elia, *Corros. Sci.* 52 (2010) 2341.
38. X.H. Li, S.D. Deng, H. Fu, *J. Appl. Electrochem.* 40 (2010) 1641.
39. I. Radojević, K. Berković, S. Kovac, J. Vorkapić-Furac, *Corros. Sci.* 50 (2008) 1498.
40. S.A. Umoren, I.B. Obot, N.O. Obi-Egbedi, *J. Mater. Sci.* (2009) 274.
41. M.I. Awad, *J. Appl. Electrochem.* 36 (2006) 1163.
42. P.C. Okafor, M.E. Ikpi, I.E. Uwah, E.E. Ebenso, U.J. Ekpe, S.A. Umoren, *Corros. Sci.* 50 (2008) 2310.
43. A.K. Satapathy, G. Gunasekaran, S.C. Sahoo, K. Amit, P.V. Rodrigues, *Corros. Sci.* 51 (2009) 2848.
44. A.M. Abdel-Gaber, B.A. Abd-El-Nabey, M. Saadawy, *Corros. Sci.* 51 (2009) 1038.
45. K.W. Tan, M.J. Kassim, *Corros. Sci.* 53 (2011) 569
46. E. H. El-Ashry, A. El-Nemir, S. A. Esawy, S. Ragab, *Electr. Acta* 51 (2006) 3957.
47. M. G. Sethuran, P. B. Raja, *Pigment & Resin Technol.* 34 (2006) 327.
48. A. Bouyanzer, L. Majidi, B. Hammouti, *Phys. Chem. News* 37 (2007) 70.
49. A. El bribri, M. Tabyaoui, H. El Attari, K. Boumhara, M. Siniti, B. Tabyaoui, *J. Mater. Environ. Sci.* 2 (2011) 156.
50. E. Chaieb, A. Bouyanzer, B. Hammouti, M. Benkaddour, *Appl. Surf. Sci.* 246 (2005) 199.
51. L. Majidi, Z. Faska, M. Znini, S. Kharchouf, A. Bouyanzer, B. Hammouti, *J. Mater. Environ. Sci.* 1 (2010) 219.
52. A. Bouyanzer, B. Hammouti, L. Majidi, *Mater. Leters.* 60 (2006) 2840.
53. A. Bouyanzer, L. Majidi, B. Hammouti, *Bull. Electrochem.* 22 (2006) 321.
54. A. Chetouani, B. Hammouti, M. Benkaddour, *Pigment & Resin Technol.* 33 (2004) 26.
55. M. Bendahou, M. Benabdellah, B. Hammouti, *Pigment & Resin Technol.* 35 (2006) 95.
56. E. Chaieb, A. Bouyanzer, B. Hammouti, M. Benkaddour, M. Berrabah, *Trans of SAEST.* 39 (2004) 58.
57. E. El-Ouariachi, J. Paolini, M. Bouklah, A. Elidrissi, A. Bouyanzer, B. Hammouti, J-M. Desjobert, J. Costa, *Acta Metall. Sin.* 23 (2010) 13.
58. O. Ouachikh, A. Bouyanzer, M. Bouklah, J-M. Desjobert, J. Costa. B. Hammouti, L. Majidi, *Surf. Rev. and Letters.* 16 (2009) 49.
59. M. Benabdellah, M. Benkaddour, B. Hammouti, M. Bendahou, A. Aouiti, *Appl. Surf. Sci.* 252 (2006) 6212.
60. A. Bouyanzer, B. Hammouti, *Pigment & Resin Technol.* 33 (2004) 287.
61. B. Zerga, M. Sfaira, Z. Rais, M. Ebn Touhami, M. Taleb, B. Hammouti, B. Imelouane, A. Elbachiri, *Mater. Tech.* 97 (2009) 297.
62. Z. Faska, L. Majidi, R. Fihi, A. Bouyanzer, B. Hammouti, *Pigment & Resin Technol.* 36 (2007) 293.
63. E. Chaieb, A. Bouyanzer, B. Hammouti, M. Benkaddour, *Appl. Surf. Sci.* 246 (2005) 199.
64. Z. Faska, A. Bellioua, M. Bouklah, L. Majidi, R. Fihi, A. Bouyanzer, B. Hammouti, *Monatsh. Chem.* 139 (2008), 1417.
65. E. Chaieb, A. Bouyanzer, B. Hammouti, M. Berrabah, *Acta. Phys. Chim. Sin.* 25 (2009)1254.
66. K. Khallouki, B. Spiegelhalder, H. Bartsch, R.W. Owen, *Afr. J. Biotechnol.* 4 (2005) 381.
67. F. Henry, L. Danoux, G. Pauly, Z. Charrouf, Use of an extract from the plant *Argania spinosa*. PatentEP1430900, (2004).

68. (a) L. Afia, R. Salghi, L. Bammou, Lh. Bazzi, B. Hammouti, L. Bazzi, *Acta Metalurg. Sinica*, 24(6) (2011); (b) L. Afia, R. Salghi, L. Bammou, El. Bazzi, B. Hammouti, L. Bazzi, A. Bouyanzer, *J. Saudi Chem. Soc.* doi:10.1016/j.jscs.2011.05.008
69. E.G. Bligh, W.J. Dyer, *Can. J. Biochem. Physio.* 137 (1959) 911.
70. DGF, Deutsche Einheitsmethoden zur Untersuchung von Fetten, Fettprodukten, Tensiden und verwandten Stoffen. Stuttgart: Wissenschaftliche Verlagsgesellschaft, (2008).
71. M. Balz, E. Schulte, H.P. Thier, *Science Technology*, 94 (1992) 209.
72. A.M. Abdel-Gaber , B.A. Abd-El-Nabey, I.M. Sidahmed, A.M. El-Zayady, M. Saadawy. *Corros. Sci.* 48 (2006) 2765.
73. L. Bammou, M. Mihit, R. Salgh, A. Bouyanzer, S.S. Al-Deyab, L. Bazzi, B. Hammouti. *Int. J. Electrochem. Sci.*, 6 (2011) 1454.
74. T. Tsuru, S. Haruyama, B. Gijutsu, *J. Jpn. Soc. Corros. Eng.* 27 (1978) 573.
75. H. Shih, H. Mansfeld, *Corros. Sci.* 29 (1989) 1235.
76. S. Martinez, M. Metikos-Hukovic, *J. Appl. Electrochem.* 33 (2003) 1137.
77. B.A. Boukamamp, *Solid State Ionics* 20 (1980) 31.
78. F. Mansfeld, *Corrosion* 36 (1981) 301.
79. J.R. Macdonald, *J. Electroanal. Chem.* 223 (1987) 25.
80. S.F. Mertens, C. Xhoffer, B.C. De Cooman, E. Temmerman, *Corrosion* 53 (1997) 381.
81. E.L. Chaieb, A. Bouyanzer, B. Hammouti, M. Benkaddour, *Appl. Surf. Sci.* 249 (2005) 183
82. M. Bouklah, A. Attayibat, S. Kertit, A. Ramdani, B. Hammouti, *Appl. Surf. Sci.* 242 (2005) 399.
83. A. Popova, E. Sokolova, S. Raicheva, M. Christov, *Corros. Sci.* 45 (2003) 33.
84. T. Szauer, A. Brandt, *Electrochim. Acta* 22 (1981) 1209.
85. S.S. Abd-El-Rehim, S.A.M. Refaey, F. Taha, M.B. Saleh, R.A. Ahmed, *J. Appl. Electrochem.* 31 (2001) 429.
86. S. Martinez, I. Stern, *Appl. Surf. Sci.* 199 (2002) 83.
87. J. Marsh, *Advanced Organic Chemistry*, third ed., Wiley Eastern, New Delhi, 1988.
88. I. Langmuir, *J. Amer. Chem. Soc.* 39 (1947) 1848.
89. M. Dahmani, A. Et-Touhami, S.S. Al-Deyab , B. Hammouti, A. Bouyanzer, *Int. J. Electrochem. Sci.*, 5 (2010) 1060.